ACS Catalysis

pubs.acs.org/acscatalysis Research Article

Activating Copper for Electrocatalytic CO_2 Reduction to Formate via Molecular Interactions

Zixu Tao, Zishan Wu, Yueshen Wu, and Hailiang Wang*

Cite This: *ACS Catal.* 2020, 10, 9271−9275

Read Online

ACCESS | Metrics & More | Article Recommendations | Supporting Information

ABSTRACT: Cu is a well-known electrocatalyst for reducing CO_2 to various products. However, unmodified Cu exhibits poor selectivity and activity for formate production. Our in situ Raman spectroscopy study detects HCOO* intermediates on the unmodified Cu surface under CO_2 electroreduction reaction conditions and confirms their reductive desorption being the rate-limiting step of producing formate. We further show that cetyltrimethylammonium bromide (CTAB) can dramatically improve the catalysis via competitive adsorption to facilitate HCOO* desorption. The Cu−CTAB interaction leads to a faradic efficiency of 82% and a 56-fold increase in partial current density for CO_2 reduction to formate at −0.5 V vs the reversible hydrogen electrode in a near-neutral aqueous solution, which is the best performance to date for unmodified Cu under ambient conditions.

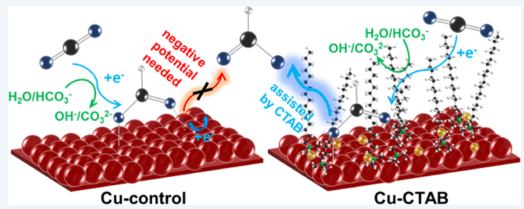

KEYWORDS: *electrochemical CO_2 reduction, in situ Raman, formate-selective, oxide-derived copper, cetyltrimethylammonium bromide (CTAB)*

Electrochemical CO_2 reduction reactions are a promising approach to the conversion of CO_2 waste to fuels and value-added chemicals.[1−11] For example, formic acid or formate, a two-electron reduction product from CO_2, is a useful chemical for the food and leather industries;[12] the reversible interconversion between formate and CO_2 can be utilized for energy storage.[13] While a number of materials have been identified to be active for catalyzing CO_2 electroreduction to formate, they fall short in one or more aspects, including activity, selectivity, durability, and cost.[14−20] As perhaps the most well-known CO_2 reduction electrocatalyst, Cu can yield different products, such as CO,[21] ethylene,[22] and ethanol,[23] with reasonable selectivity. However, Cu is not selective for CO_2 reduction to formate[24] unless modified by another element, such as S[16,25] or Sn.[26,27]

Interactions between molecular/polymeric species and material surface are emerging as a new paradigm for improving the catalytic selectivity and activity in electrochemical CO_2 reduction reactions.[28−34] The faradic efficiency (FE) of producing ethylene from CO_2 reduction was enhanced from 13 to 26% by modifying Cu foam with poly(acrylamide);[29] polyaniline coating on Cu nanoparticles was demonstrated to increase the selectivity of CO_2 electroreduction to C_{2+} products from 46.7 to nearly 80%;[31] glycine modification of Cu nanowire films was hypothesized to stabilize the *CHO intermediate and doubled the FE of total hydrocarbons.[34] These encouraging results highlight the power of material−molecule interactions for boosting the electrocatalytic CO_2 conversion, which warrants further investigation into the underlying mechanisms and other schemes that enable different products such as formate.

Herein, we present a discovery of cetyltrimethylammonium bromide (CTAB) imparting Cu with unprecedented catalytic activity and selectivity in its kind for electrochemical CO_2 reduction to formate. With CTAB added in the electrolyte, our oxide-derived Cu catalyst achieves >80% selectivity (all selectivity values are based on FE unless otherwise noted) of formate at an electrode potential of −0.5 V vs the reversible hydrogen electrode (RHE; all potentials are referenced to the RHE scale unless otherwise noted). At this potential, the presence of CTAB improves the CO_2-to-formate conversion rate by 56 times. In situ Raman spectroscopy study for the first time identifies HCOO* reaction intermediates on the unmodified Cu surface under CO_2 electroreduction conditions. Under reaction conditions, CTAB accelerates the rate-limiting HCOO* desorption step via competitive adsorption on Cu sites, leading to enhanced CO_2 reduction to formate.

The Cu catalyst was prepared in situ from electrochemically reducing 8 nm size CuO nanoparticles synthesized following a prior work (see the Supporting Information for experimental details).[35] Loaded on a carbon fiber paper and tested in a CO_2-saturated 0.5 M $KHCO_3$ aqueous electrolyte, the catalyst exhibited potential-dependent product selectivity (Figure 1a; see Figure S1 for current density information). H_2 evolution

Received: May 21, 2020
Revised: July 21, 2020
Published: July 22, 2020

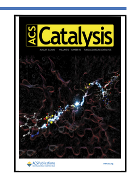

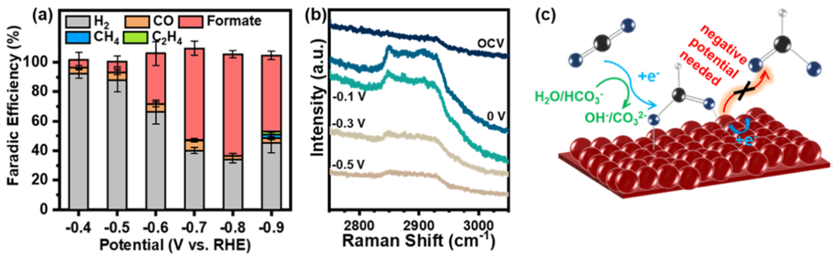

Figure 1. CO_2 reduction electrocatalysis of oxide-derived Cu in the CO_2-saturated 0.5 M aqueous $KHCO_3$. (a) Potential-dependent product distribution (FE). (b) In situ Raman spectra at different applied potentials. (c) Schematic illustration of the reaction pathway.

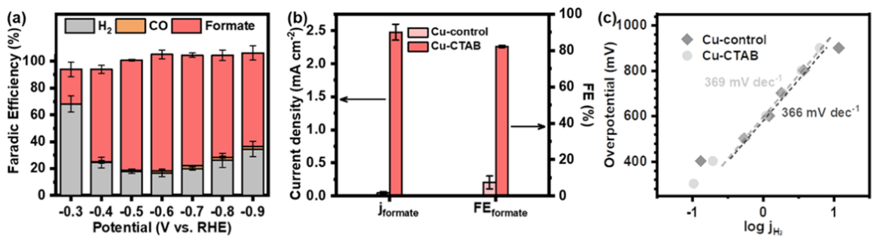

Figure 2. (a) CO_2 reduction performance of Cu−CTAB in the CO_2-saturated 0.5 M $KHCO_3$: potential-dependent product distribution (FE). (b) Comparison of the electrocatalytic performance with and without CTAB at −0.5 V: partial current density and FE. (c) Tafel plots of H_2 evolution for the Cu catalyst with and without CTAB in the CO_2-saturated 0.5 M $KHCO_3$.

accounts for the majority of the reduction current between −0.4 and −0.6 V. Formate is a minor product in this range. At more negative working electrode potentials, formate is the major product, with the highest FE of 69% reached at −0.8 V. CH_4 and C_2H_4 emerge as minor products at −0.9 V. CO is generated in the entire potential range studied, but all with less than 7% selectivity.

Surface species on the Cu catalyst was studied by in situ Raman spectroscopy under electrochemical CO_2 reduction conditions (Figure S2). A band centered at approximately 2900 cm^{-1} was observed in the potential window of 0 to −0.5 V (Figure 1b), which we assign to the C−H stretching of surface-adsorbed HCOO species (HCOO*), a reaction intermediate in CO_2 electroreduction to formate. The same intermediate has been observed under ultrahigh vacuum conditions,[36] in thermal catalysis,[37,38] and in the process of electrochemical oxidation of formic acid on metal surfaces.[25,39] We also observed this vibrational band on our Cu catalyst under electrochemical conditions in an Ar-purged electrolyte containing 10 mM HCOOK (Figure S3a). To verify that this HCOO* is an intermediate from CO_2 reduction, we investigated our Cu catalyst in an Ar-purged 0.1 M $KClO_4$ aqueous solution and found no presence of HCOO* in the potential range of 0 to −0.5 V; when CO_2 was introduced in the system, HCOO* was readily detected (Figure S3b).

The presence of HCOO* intermediates on the Cu surface in the low overpotential range, where formate is not observed in the products, suggests that its reductive desorption to form free formate is likely the rate-limiting step (Figure 1c). The coverage of HCOO* decreases at more negative electrode potentials (Figure 1b), probably because negative potentials facilitate reductive desorption. Consistently, formate production occurs at −0.4 V, and the rate increases at more negative potentials (Figure S1). In fact, density functional theory calculations have suggested that HCOO* binds to the Cu surface strongly and thus its desorption is the potential-limiting step for CO_2 electroreduction to formate.[26,39] To the best of our knowledge, our results provide the first experimental evidence for HCOO* from CO_2 electroreduction on the unmodified Cu surface supporting these theoretical predictions. Given that CO_2 can be converted to HCOO* at potentials as positive as 0 V, which is near the thermodynamic potential of the CO_2/formate redox pair, Cu has the potential to become a highly active electrocatalyst for producing formate from CO_2 if the HCOO* desorption step can be accelerated.

We found that the catalytic performance of the Cu electrocatalyst for formate production from CO_2 can be drastically enhanced by incorporating CTAB. In the presence of 0.167 mM CTAB dissolved in the electrolyte, the Cu catalyst (denoted as Cu−CTAB in this case) shows an increased current density from −0.3 to −0.8 V compared to the Cu−control case without the CTAB additive (Figure S1); it starts to generate formate at −0.3 V with an FE of 26%, which increases to 69% at −0.4 V and over 80% from −0.5 to −0.7 V (Figure 2a). Cu−CTAB reaches 82.3% of $FE_{formate}$ and 2.48 mA cm^{-2} of $j_{formate}$ at −0.5 V, which is 11-fold more selective and 56-fold more active than the Cu−control at the same electrode potential (Figure 2b). This is arguably the highest catalytic performance for CO_2 electroreduction to formate reported to date for unmodified Cu under ambient conditions (Table S1). This CTAB-activated formate production is stable for hours of operation. In a 10 h electrolysis at −0.5 V, the final current was 96% of the initial value, and an average formate selectivity of 88.2% was achieved (Figure S4). Without CO_2 feeding, Cu−CTAB only generates H_2 across the potential range in an Ar-purged electrolyte (Figure S5), proving that CTAB is assisting with CO_2 reduction rather than releasing formate from its own decomposition. As we lower the concentration of CTAB, the enhancement becomes less pronounced but is still significant (Figure S6). As a direct competing reaction of CO_2 reduction, H_2 evolution was also examined. Interestingly, we found that both the partial current densities and Tafel slopes are almost identical for the two cases with and without the presence of CTAB (Figure 2c). This suggests that CTAB does not alter the reaction rate or pathway of H_2 evolution, which to some degree contradicts a previous

https://dx.doi.org/10.1021/acscatal.0c02237
ACS Catal. 2020, 10, 9271−9275

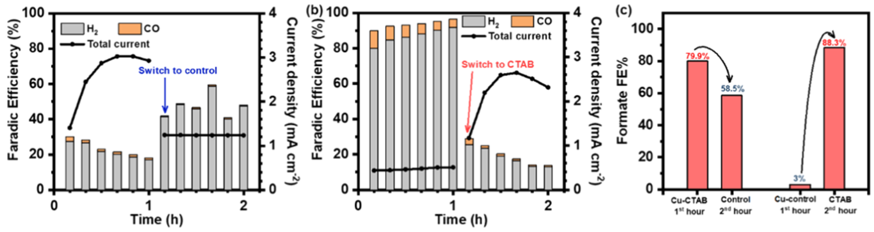

Figure 3. Electrolyte-switching experiments at −0.5 V: (a) CTAB-containing and then CTAB-free conditions; (b) CTAB-free and then CTAB-containing conditions; and (c) $FE_{formate}$ for processes shown in (a) and (b).

report that CTAB suppresses H_2 evolution on Cu,[30] although we do note that the polycrystalline Cu substrate used in that study and the oxide-derived Cu in this study can behave quite differently in electrocatalytic CO_2 reduction, as shown by prior reports.[24,40,41] This result further implies that the active sites of Cu−control and Cu−CTAB are the same and that CTAB promotes CO_2 reduction to formate via a different scheme than modifying the Cu sites.

The two Cu catalysts prereduced in electrolytes with and without CTAB were characterized by multiple techniques. X-ray diffraction (XRD) and scanning electron microscopy (SEM) show that both samples consist of only the metallic Cu phase (Figure S7a) with a similar morphology of coalesced particles (Figure S7b,c). X-ray photoelectron spectroscopy (XPS) with a protected sample transfer[35,42,43] reveals that Cu^{2+} from the original CuO nanoparticles has been fully reduced regardless of whether CTAB is present (Figure S7d), and the Cu LMM Auger spectra indicate that both catalyst surfaces are dominated by Cu^0 (Figure S7e). Regardless of the CTAB's presence, Raman spectroscopic measurements under electrochemical CO_2 reduction conditions identify Cu_2O species on the surface at the open-circuit potential, which disappears as a reductive electrode potential is applied (Figure S8). These results suggest that the Cu−CTAB interactions do not alter the microstructure or oxidation state of the Cu catalyst, supporting our prior postulation based on the H_2 evolution rates.

Control experiments also support the conclusion that CTAB does not modify the Cu sites but might directly interact with the CO_2 reduction process. This hypothesis is supported by electrolyte-switching measurements. In the first electrolyte-switching experiment, after performing CO_2 reduction to formate for 1 h with an average FE of 80% in a CTAB-containing electrolyte, the Cu catalyst was transferred to a fresh electrolyte without CTAB. A substantial decay in the catalytic efficacy in terms of both $j_{formate}$ and $FE_{formate}$ was observed (Figure 3a,c). This excludes the possibility that CTAB improves the catalysis by permanently restructuring the Cu catalyst. Note that in the successive electrolysis in the fresh electrolyte, the reused Cu catalyst is more active and selective for producing formate than a fresh Cu catalyst because of the CTAB residue on the working electrode from the previous electrolysis. Consistently, in the second electrolyte-switching experiment, $FE_{formate}$ climbed from 3 to 88% in conjunction with an increase in current density as the Cu catalyst electrode was transferred from a CTAB-free electrolyte to a CTAB-containing electrolyte (Figure 3b,c).

To further understand how CTAB promotes CO_2 reduction to formate on Cu, we carried out in situ Raman spectroscopy studies. Similar to the Cu−control case, a band centered at 2900 cm^{-1} pertaining to HCOO* was observed on Cu−CTAB at 0 V (Figure 4a). As the electrode potential was shifted

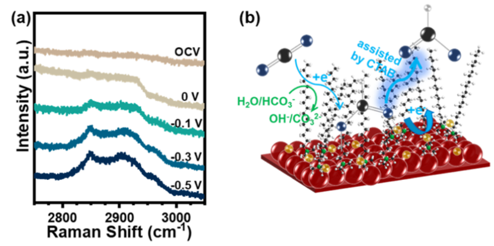

Figure 4. (a) In situ Raman spectra of Cu−CTAB in the CO_2-saturated 0.5 M $KHCO_3$ under applied potentials. (b) Schematic illustration of the CTAB-assisted electrochemical CO_2 reduction to formate on Cu.

toward the more negative direction, this band changed its shape and grew its intensity, implying an increasing surface coverage of a different species. We believe that this species is CTA^+ because it possesses an identical C−H vibrational band at 2900 cm^{-1} as pure CTAB (Figure S9a) and its adsorption on the Cu surface increases at more negative potentials (Figure S9b), which agrees with our expectation for a positively charged cationic species. Given these spectral changes and our prior observation that HCOO* desorption is the rate-limiting step, we postulate that CTAB effectively boosts CO_2 reduction to formate by displacing HCOO* on the Cu surface (Figure 4b). This also agrees with our Tafel analysis. Both Cu−control and Cu−CTAB exhibit a Tafel slope of approximately 110 mV dec^{-1} in the mid-overpotential range despite a 200 mV overpotential reduction caused by CTAB (Figure S10a), which implies that the reaction steps involving electron transfer before the rate-limiting step are barely affected by CTAB. This Tafel slope value is consistent with a hypothetical reaction mechanism assuming a high surface coverage of H* and HCOO* desorption being the rate-liming step (see Supporting Information for details). We also note that the enhancing effects from CTAB are less prominent at potentials more negative than −0.5 V and disappears at −0.9 V (Figure S10b) even though the surface coverage of CTAB is supposed to be higher at more negative potentials (Figures 4a and S9b). This can be explained by the fact that HCOO* desorption from the Cu surface is already activated by the sufficiently negative potentials in these conditions.

Finally, we varied the cation and anion parts of CTAB and investigated their influences on the catalysis. Interestingly, the cation and anion appear to contribute to the enhanced catalytic activity in different ways. On the one hand, both the FE and partial current density for formate decrease significantly as we shorten the straight-chain alkyl group R of the $NR(CH_3)_3Br$ additive from C_{16} to C_{14} and to C_{12} (Figure 5a); when R is shorter than C_{12}, no enhancement over the Cu−control case without any additive can be concluded. This indicates that the effectiveness of the cation displacing HCOO* may be related

https://dx.doi.org/10.1021/acscatal.0c02237
ACS Catal. 2020, 10, 9271−9275

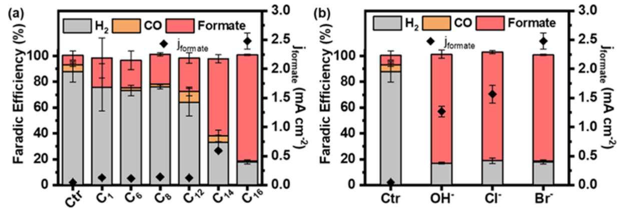

Figure 5. Dependence of the electrocatalytic CO_2 reduction performance of Cu on (a) straight-chain alkyl group R of the $NR(CH_3)_3Br$ additive and (b) anion of the CTA^+ additive measured by 1 h electrolysis at −0.5 V. The controls were measured in an additive-free electrolyte.

to its size[44] or other factors such as hydrophobicity, which warrants further investigation. On the other hand, the identity of the anion for the CTA^+ additive does not affect $FE_{formate}$ but seems to be correlated with $j_{formate}$: despite similarly high $FE_{formate}$, $j_{formate}$ for OH^- or Cl^- is considerably lower than that for Br^- (Figure 5b). This anion effect might be related to the Cu−halide interaction, which has been demonstrated to induce nanostructuring and enhance CO_2 reduction to C_2–C_3 products,[45,46] which also needs further investigation. We note that the morphology of the Cu catalyst revealed by SEM (Figure S11) and the relative surface area measured from the non-faradic charge adsorption process (Figure S12) do not seem to depend on the anion identity.

In summary, we have discovered that adding CTAB to the electrolyte can make unmodified Cu a highly active and selective catalyst for formate production from electrochemical CO_2 reduction, achieving an 82% formate selectivity and a 56-fold increase in partial current density at −0.5 V vs RHE in a near-neutral aqueous electrolyte. The enhancement is originated from the CTAB−Cu interaction which facilitates the rate-limiting HCOO* desorption step in the CO_2 reduction process.

■ ASSOCIATED CONTENT

Supporting Information

The Supporting Information is available free of charge at https://pubs.acs.org/doi/10.1021/acscatal.0c02237.

Experimental details, Tafel analysis, and supplementary table and figures (PDF)

■ AUTHOR INFORMATION

Corresponding Author

Hailiang Wang − *Department of Chemistry and Energy Sciences Institute, Yale University, New Haven, Connecticut 06520, United States;* orcid.org/0000-0003-4409-2034; Email: hailiang.wang@yale.edu

Authors

Zixu Tao − *Department of Chemistry and Energy Sciences Institute, Yale University, New Haven, Connecticut 06520, United States*

Zishan Wu − *Department of Chemistry and Energy Sciences Institute, Yale University, New Haven, Connecticut 06520, United States;* orcid.org/0000-0003-4810-9112

Yueshen Wu − *Department of Chemistry and Energy Sciences Institute, Yale University, New Haven, Connecticut 06520, United States*

Complete contact information is available at: https://pubs.acs.org/10.1021/acscatal.0c02237

Notes

The authors declare no competing financial interest.

■ ACKNOWLEDGMENTS

This work was supported by the National Science Foundation (Grant CHE-1651717). Z.T. acknowledges support from the Tully Graduate Research Fellowship in Chemistry from Yale University. H.W. acknowledges support from the Sloan Research Fellowship.

■ REFERENCES

(1) Kuhl, K. P.; Hatsukade, T.; Cave, E. R.; Abram, D. N.; Kibsgaard, J.; Jaramillo, T. F. Electrocatalytic Conversion of Carbon Dioxide to Methane and Methanol on Transition Metal Surfaces. *J. Am. Chem. Soc.* **2014**, *136*, 14107−14113.

(2) Larrazábal, G. O.; Martin, A. J.; Perez-Ramirez, J. Building Blocks for High Performance in Electrocatalytic CO_2 Reduction: Materials, Optimization Strategies, and Device Engineering. *J. Phys. Chem. Lett.* **2017**, *8*, 3933−3944.

(3) Duan, X.; Xu, J.; Wei, Z.; Ma, J.; Guo, S.; Wang, S.; Liu, H.; Dou, S. Metal-Free Carbon Materials for CO_2 Electrochemical Reduction. *Adv. Mater.* **2017**, *29*, No. 1701784.

(4) Artz, J.; Muller, T. E.; Thenert, K.; Kleinekorte, J.; Meys, R.; Sternberg, A.; Bardow, A.; Leitner, W. Sustainable Conversion of Carbon Dioxide: An Integrated Review of Catalysis and Life Cycle Assessment. *Chem. Rev.* **2018**, *118*, 434−504.

(5) Thonemann, N.; Pizzol, M. Consequential Life Cycle Assessment of Carbon Capture and Utilization Technologies within the Chemical Industry. *Energy Environ. Sci.* **2019**, *12*, 2253−2263.

(6) Huo, S.; Weng, Z.; Wu, Z.; Zhong, Y.; Wu, Y.; Fang, J.; Wang, H. Coupled Metal/Oxide Catalysts with Tunable Product Selectivity for Electrocatalytic CO_2 Reduction. *ACS Appl. Mater. Interfaces* **2017**, *9*, 28519−28526.

(7) Wu, Y.; Jiang, Z.; Lu, X.; Liang, Y.; Wang, H. Domino Electroreduction of CO_2 to Methanol on a Molecular Catalyst. *Nature* **2019**, *575*, 639−642.

(8) Cai, Z.; Wu, Y.; Wu, Z.; Yin, L.; Weng, Z.; Zhong, Y.; Xu, W.; Sun, X.; Wang, H. Unlocking Bifunctional Electrocatalytic Activity for CO_2 Reduction Reaction by Win-Win Metal−Oxide Cooperation. *ACS Energy Lett.* **2018**, *3*, 2816−2822.

(9) Weng, Z.; Jiang, J.; Wu, Y.; Wu, Z.; Guo, X.; Materna, K. L.; Liu, W.; Batista, V. S.; Brudvig, G. W.; Wang, H. Electrochemical CO_2 Reduction to Hydrocarbons on a Heterogeneous Molecular Cu Catalyst in Aqueous Solution. *J. Am. Chem. Soc.* **2016**, *138*, 8076−8079.

(10) Weng, Z.; Wu, Y.; Wang, M.; Jiang, J.; Yang, K.; Huo, S.; Wang, X. F.; Ma, Q.; Brudvig, G. W.; Batista, V. S.; Liang, Y.; Feng, Z.; Wang, H. Active Sites of Copper-Complex Catalytic Materials for Electrochemical Carbon Dioxide Reduction. *Nat. Commun.* **2018**, *9*, No. 415.

(11) Weng, Z.; Zhang, X.; Wu, Y.; Huo, S.; Jiang, J.; Liu, W.; He, G.; Liang, Y.; Wang, H. Self-Cleaning Catalyst Electrodes for Stabilized CO_2 Reduction to Hydrocarbons. *Angew. Chem., Int. Ed.* **2017**, *56*, 13135−13139.

(12) Bulushev, D. A.; Ross, J. R. H. Towards Sustainable Production of Formic Acid. *ChemSusChem* **2018**, *11*, 821−836.

(13) Lu, X.; Wu, Y.; Yuan, X.; Wang, H. An Integrated CO_2 Electrolyzer and Formate Fuel Cell Enabled by a Reversibly Restructuring Pb-Pd Bimetallic Catalyst. *Angew. Chem., Int. Ed.* **2019**, *58*, 4031−4035.

(14) Chatterjee, S.; Griego, C.; Hart, J. L.; Li, Y.; Taheri, M. L.; Keith, J.; Snyder, J. D. Free Standing Nanoporous Palladium Alloys as CO Poisoning Tolerant Electrocatalysts for the Electrochemical Reduction of CO_2 to Formate. *ACS Catal.* **2019**, *9*, 5290−5301.

(15) Lee, C. H.; Kanan, M. W. Controlling H^+ vs CO_2 Reduction Selectivity on Pb Electrodes. *ACS Catal.* **2015**, *5*, 465−469.

(16) Shinagawa, T.; Larrazabal, G. O.; Martin, A. J.; Krumeich, F.; Perez-Ramirez, J. Sulfur-Modified Copper Catalysts for the Electro-

chemical Reduction of Carbon Dioxide to Formate. *ACS Catal.* **2018**, *8*, 837−844.
(17) Bai, X.; Chen, W.; Zhao, C.; Li, S.; Song, Y.; Ge, R.; Wei, W.; Sun, Y. Exclusive Formation of Formic Acid from CO_2 Electroreduction by a Tunable Pd-Sn Alloy. *Angew. Chem., Int. Ed.* **2017**, *56*, 12219−12223.
(18) Han, N.; Wang, Y.; Yang, H.; Deng, J.; Wu, J.; Li, Y.; Li, Y. Ultrathin Bismuth Nanosheets from In Situ Topotactic Transformation for Selective Electrocatalytic CO_2 Reduction to Formate. *Nat. Commun.* **2018**, *9*, No. 1320.
(19) Ma, W.; Xie, S.; Zhang, X. G.; Sun, F.; Kang, J.; Jiang, Z.; Zhang, Q.; Wu, D. Y.; Wang, Y. Promoting Electrocatalytic CO_2 Reduction to Formate via Sulfur-Boosting Water Activation on Indium Surfaces. *Nat. Commun.* **2019**, *10*, No. 892.
(20) Gao, S.; Lin, Y.; Jiao, X.; Sun, Y.; Luo, Q.; Zhang, W.; Li, D.; Yang, J.; Xie, Y. Partially Oxidized Atomic Cobalt Layers for Carbon Dioxide Electroreduction to Liquid Fuel. *Nature* **2016**, *529*, 68−71.
(21) Raciti, D.; Livi, K. J.; Wang, C. Highly Dense Cu Nanowires for Low-Overpotential CO_2 Reduction. *Nano Lett.* **2015**, *15*, 6829−6835.
(22) Mistry, H.; Varela, A. S.; Bonifacio, C. S.; Zegkinoglou, I.; Sinev, I.; Choi, Y.-W.; Kisslinger, K.; Stach, E. A.; Yang, J. C.; Strasser, P.; Cuenya, B. R. Highly Selective Plasma-Activated Copper Catalysts for Carbon Dioxide Reduction to Ethylene. *Nat. Commun.* **2016**, *7*, No. 12123.
(23) Morales-Guio, C. G.; Cave, E. R.; Nitopi, S. A.; Feaster, J. T.; Wang, L.; Kuhl, K. P.; Jackson, A.; Johnson, N. C.; Abram, D. N.; Hatsukade, T.; Hahn, C.; Jaramillo, T. F. Improved CO_2 Reduction Activity towards C_{2+} Alcohols on a Tandem Gold on Copper Electrocatalyst. *Nat. Catal.* **2018**, *1*, 764−771.
(24) Li, C. W.; Kanan, M. W. CO_2 Reduction at Low Overpotential on Cu Electrodes Resulting from the Reduction of Thick Cu_2O Films. *J. Am. Chem. Soc.* **2012**, *134*, 7231−7234.
(25) Pan, Z.; Wang, K.; Ye, K.; Wang, Y.; Su, H.-Y.; Hu, B.; Xiao, J.; Yu, T.; Wang, Y.; Song, S. Intermediate Adsorption States Switch to Selectively Catalyze Electrochemical CO_2 Reduction. *ACS Catal.* **2020**, *10*, 3871−3880.
(26) Zheng, X.; Ji, Y.; Tang, J.; Wang, J.; Liu, B.; Steinrück, H.-G.; Lim, K.; Li, Y.; Toney, M. F.; Chan, K.; Cui, Y. Theory-Guided Sn/Cu Alloying for Efficient CO_2 Electroreduction at Low Overpotentials. *Nat. Catal.* **2019**, *2*, 55−61.
(27) Vasileff, A.; Zhi, X.; Xu, C.; Ge, L.; Jiao, Y.; Zheng, Y.; Qiao, S. Z. Selectivity Control for Electrochemical CO_2 Reduction by Charge Redistribution on the Surface of Copper Alloys. *ACS Catal.* **2019**, *9*, 9411−9417.
(28) Wagner, A.; Ly, K. H.; Heidary, N.; Szabo, I.; Foldes, T.; Assaf, K. I.; Barrow, S. J.; Sokolowski, K.; Al-Hada, M.; Kornienko, N.; Kuehnel, M. F.; Rosta, E.; Zebger, I.; Nau, W. M.; Scherman, O. A.; Reisner, E. Host-Guest Chemistry Meets Electrocatalysis: Cucurbit[6]uril on a Au Surface as a Hybrid System in CO_2 Reduction. *ACS Catal.* **2020**, *10*, 751−761.
(29) Ahn, S.; Klyukin, K.; Wakeham, R. J.; Rudd, J. A.; Lewis, A. R.; Alexander, S.; Carla, F.; Alexandrov, V.; Andreoli, E. Poly-Amide Modified Copper Foam Electrodes for Enhanced Electrochemical Reduction of Carbon Dioxide. *ACS Catal.* **2018**, *8*, 4132−4142.
(30) Banerjee, S.; Han, X.; Thoi, V. S. Modulating the Electrode−Electrolyte Interface with Cationic Surfactants in Carbon Dioxide Reduction. *ACS Catal.* **2019**, *9*, 5631−5637.
(31) Wei, X.; Yin, Z.; Lyu, K.; Li, Z.; Gong, J.; Wang, G.; Xiao, L.; Lu, J.; Zhuang, L. Highly Selective Reduction of CO_2 to C_{2+} Hydrocarbons at Copper/Polyaniline Interfaces. *ACS Catal.* **2020**, *10*, 4103−4111.
(32) Han, Z.; Kortlever, R.; Chen, H. Y.; Peters, J. C.; Agapie, T. CO2 Reduction Selective for C>/=2 Products on Polycrystalline Copper with N-Substituted Pyridinium Additives. *ACS Cent. Sci.* **2017**, *3*, 853−859.
(33) Quan, F.; Xiong, M.; Jia, F.; Zhang, L. Efficient Electroreduction of CO_2 on Bulk Silver Electrode in Aqueous Solution via the Inhibition of Hydrogen Evolution. *Appl. Surf. Sci.* **2017**, *399*, 48−54.
(34) Xie, M. S.; Xia, B. Y.; Li, Y.; Yan, Y.; Yang, Y.; Sun, Q.; Chan, S. H.; Fisher, A.; Wang, X. Amino acid modified copper electrodes for the enhanced selective electroreduction of carbon dioxide towards hydrocarbons. *Energy Environ. Sci.* **2016**, *9*, 1687−1695.
(35) Tao, Z.; Wu, Z.; Yuan, X.; Wu, Y.; Wang, H. Copper Gold Interactions Enhancing Formate Production from Electrochemical CO_2 Reduction. *ACS Catal.* **2019**, *9*, 10894−10898.
(36) Pohl, M.; Pieck, A.; Hanewinkel, C.; Otto, A. Raman Study of Formic Acid and Surface Formate Adsorbed on Cold-Deposited Copper Films. *J. Raman Spectrosc.* **1996**, *27*, 805−809.
(37) Bando, K. K.; Sayama, K.; Kusama, H.; Okabe, K.; Arakawa, H. In-situ FT-IR study on CO_2 hydrogenation over Cu catalysts supported on SiO_2, Al_2O_3, and TiO_2. *Appl. Catal., A* **1997**, *165*, 391−409.
(38) Nakamura, I.; Nakano, H.; Fujitani, T.; Uchijima, T.; Nakamura, J. Evidence for a special formate species adsorbed on the Cu-Zn active site for methanol synthesis. *Surf. Sci.* **1998**, *402*−*404*, 92−95.
(39) Deng, Y.; Huang, Y.; Ren, D.; Handoko, A. D.; Seh, Z. W.; Hirunsit, P.; Yeo, B. S. On the Role of Sulfur for the Selective Electrochemical Reduction of CO_2 to Formate on CuS_X Catalysts. *ACS Appl. Mater. Interfaces* **2018**, *10*, 28572−28581.
(40) Lei, Q.; Zhu, H.; Song, K.; Wei, N.; Liu, L.; Zhang, D.; Yin, J.; Dong, X.; Yao, K.; Wang, N.; Li, X.; Davaasuren, B.; Wang, J.; Han, Y. Investigating the Origin of Enhanced C_{2+} Selectivity in Oxide-/Hydroxide-Derived Copper Electrodes during CO_2 Electroreduction. *J. Am. Chem. Soc.* **2020**, *142*, 4213−4222.
(41) Yang, P. P.; Zhang, X. L.; Gao, F. Y.; Zheng, Y. R.; Niu, Z. Z.; Yu, X.; Liu, R.; Wu, Z. Z.; Qin, S.; Chi, L. P.; Duan, Y.; Ma, T.; Zheng, X. S.; Zhu, J. F.; Wang, H. J.; Gao, M. R.; Yu, S. H. Protecting Copper Oxidation State via Intermediate Confinement for Selective CO_2 Electroreduction to C_{2+} Fuels. *J. Am. Chem. Soc.* **2020**, *142*, 6400−6408.
(42) Wu, Z.; Huang, L.; Liu, H.; Wang, H. Element-Specific Restructuring of Anion- and Cation-Substituted Cobalt Phosphide Nanoparticles under Electrochemical Water-Splitting Conditions. *ACS Catal.* **2019**, *9*, 2956−2961.
(43) Wu, Z.; Li, X.; Liu, W.; Zhong, Y.; Gan, Q.; Li, X.; Wang, H. Materials Chemistry of Iron Phosphosulfide Nanoparticles: Synthesis, Solid State Chemistry, Surface Structure, and Electrocatalysis for the Hydrogen Evolution Reaction. *ACS Catal.* **2017**, *7*, 4026−4032.
(44) Li, J.; Li, X.; Gunathunge, C. M.; Waegele, M. M. Hydrogen Bonding Steers the Product Selectivity of Electrocatalytic CO Reduction. *Proc. Natl. Acad. Sci. U.S.A.* **2019**, *116*, 9220−9229.
(45) Gao, D.; Scholten, F.; Roldan Cuenya, B. Improved CO_2 Electroreduction Performance on Plasma-Activated Cu Catalysts via Electrolyte Design: Halide Effect. *ACS Catal.* **2017**, *7*, 5112−5120.
(46) Varela, A. S.; Ju, W.; Reier, T.; Strasser, P. Tuning the Catalytic Activity and Selectivity of Cu for CO_2 Electroreduction in the Presence of Halides. *ACS Catal.* **2016**, *6*, 2136−2144.